332 | November 1975

SCHRIFTENREIHE SCHIFFBAU

Werner Blendermann

On a Probabilistic Approach to the Influence of Wind on the Longitudinal Ventilation of Road Tunnels

TUHH
Technische Universität Hamburg-Harburg

On a Probabilistic Approach to the Influence of Wind on the Longitudinal Ventilation of Road Tunnels

Werner Blendermann

Hamburg, Technische Universität Hamburg-Harburg, 1975

Schriftenreihe Schiffbau
Schwarzenbergstraße 95c
D-21073 Hamburg

http://www.tuhh.de/vss

INSTITUT FÜR SCHIFFBAU
DER UNIVERSITÄT HAMBURG

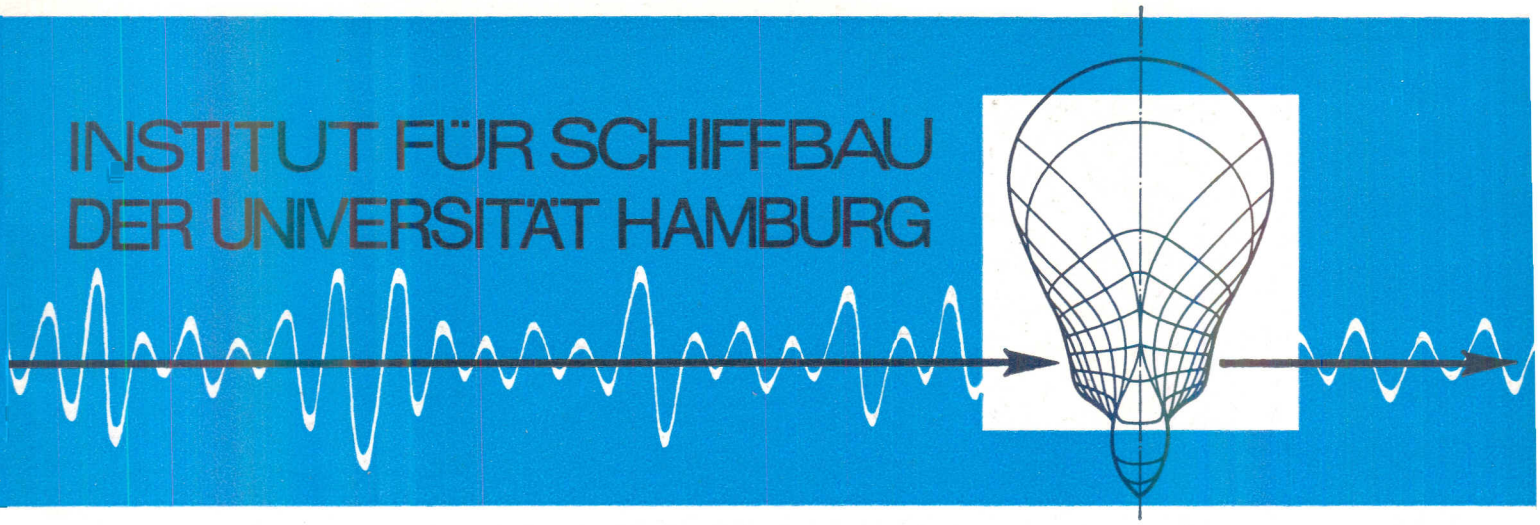

On a Probabilistic Approach to the Influence of Wind on the Longitudinal Ventilation of Road Tunnels

Werner Blendermann

November 1975

Bericht Nr. 332

INSTITUT FÜR SCHIFFBAU DER UNIVERSITÄT HAMBURG

Bericht Nr. 332

November 1975

ON A PROBABILISTIC APPROACH TO THE INFLUENCE OF WIND ON THE LONGITUDINAL VENTILATION OF ROAD TUNNELS

Werner Blendermann

SUMMARY

Wind tunnel tests on typical portals of a two-bore road tunnel demonstrated that the wind pressure differences along a tunnel can be described approximately by the $\cos^2$ of the angle of wind incidence with respect to the tunnel axis. If, then, the density curve of wind velocities is substituted by Rayleigh's density function, and if further a weighted mean wind velocity is chosen in the sector of positive or negative wind influence, the density curve of the wind pressure differences (as a function of the wind component in tunnel direction) resembles the normal density function. With this approach the wind influence on tunnel ventilation can be calculated as a free probabilistic parameter together with the aerodynamic equations of tunnel ventilation.

Prepared for

SECOND INTERNATIONAL SYMPOSIUM ON THE AERODYNAMICS AND VENTILATION OF VEHICLE TUNNELS
Churchill College, Cambridge, U.K., March 23-25, 1976

TABLE OF CONTENTS

NOMENCLATURE

A_c	projected frontal area of vehicle
A_t	tunnel cross-sectional area
C	non-dimensional quantity for abbreviation
c	wind pressure coefficient
$\bar{c}$	mean wind pressure coefficient
$\overline{c_c A_c}$	mean drag area of vehicle in tunnel
co	CO concentration
co_i	imaginary CO concentration for $v_t = v_c$
co_d	CO concentration for $n_{c,max}$, without wind influence
F	distribution function
f	density function
n_c	number of vehicles
$n_{c,max}$	maximum number of vehicles
n_j, N_j	number of axial fans
P	probability of occurrence
Δp	wind pressure difference
Q_j	volume flow rate of axial fan
$\bar{Q}_{CO}$	mean volume flow rate of carbon monoxide exhaust of vehicle
v	wind velocity
$\bar{v}$	mean wind velocity
v_c	traffic speed
v_j	jet velocity of axial fan
v_p	wind influence velocity
$\bar{v}_p$	mean wind influence velocity
v_t	longitudinal air stream velocity in tunnel, positive in the direction of traffic flow
$v_{t,max}$	maximum longitudinal air stream velocity in tunnel
$\bar{\alpha} = \overline{c_c A_c}/A_t$	mean drag area of vehicle in tunnel related to tunnel cross-sectional area

ζ_c, ζ_p	non-dimensional quantities for abbreviation
ζ_t	bulk loss coefficient of tunnel
$\mu = v_p/\bar{v}_p$	wind influence velocity related to mean wind influence velocity
$\nu = n_c/n_{c,max}$	number of vehicles related to maximum number of vehicles
ρ	air density
$\sigma = co/co_i$	CO concentration related to imaginary CO concentration
ϕ	standardized normal distribution
φ	angle of wind incidence with respect to tunnel axis
ψ	wind direction

1. INTRODUCTION

The action of wind on road tunnel ventilation can be favourable or unfavourable. In the case of retarding wind pressure differences, possibly additional ventilation boost is needed to prevent the air quality from sinking beneath certain limiting values inside the tunnel and at its ends. Since the design traffic situation for which the ventilation system is dimensioned (generally congested traffic, or stationary vehicles with idling engines) can coincide with unfavourable winds, a certain margin of ventilation boost based on a deterministic consideration of the wind effects, is often provided for.

Hitherto, there is obviously a gap in our knowledge of the general statistical response of tunnel ventilation to wind action. In this paper a probabilistic approach for the wind effects on tunnel ventilation, based on wind tunnel tests, is proposed. It can be applied especially to longitudinal ventilation systems to avoid undesirable situations.

2. WIND TUNNEL TESTS

The prospect of giving a satisfactory prediction of the influence of wind, varying at random in speed and direction, on road tunnels must seem poor at first glance because of the variety of shapes of tunnel portals. Moreover, their immediate surroundings vary so much, that the same wind pressure dependence can hardly be expected for two differing situations. On the other hand, when one regards the wind effect as a random influence, details in the wind pressure curve as a function of wind direction are less important.

The general behavior of wind action has not been investigated so far. To take up the problem, wind tunnel tests on small-scale models (1:200) of portals of a two-bore tunnel were performed at the *Institut für Schiffbau der Universität Hamburg*. In view of the complexity of the actual conditions, we confined ourselves to tunnel portals without any surrounding buildings or other obstructions.

Three basic generic shapes of a tunnel portal, selected as guide-line configurations, were tested which can be characterized shortly as follows:

- portal at ground level
- portal below ground level, with vertical side-walls
- portal below ground level, with sloping bounds (1:1)

These models could be modified by a dividing wall between the roadways (preventing recirculation of contaminated air), a light adaptation section, and by an additional transverse dam above the tunnel portal. In this way 16 different models were generated, as shown in the following table.

additional device	portal above ground level	portal below ground level, with vertical side-walls	with sloping bounds
--	* (Fig. 1a)	* (Fig. 1d)	*
dividing wall	* (Fig. 1b)	* (Fig. 1e)	*
light adaptation section	* (Fig. 1c)	* (Fig. 1f)	
dam	*	*	* (Fig. 1g)
dividing wall, dam	*	*	*
light adaptation section, dam	*	*	

The tunnel cross-section was chosen rectangular with dimensions of road tunnels for double-lane highways with an additional safety lane (Fig. 2). The tunnel tubes were made air-tight.

Portals with carriageways at ground level are sometimes found e.g. at airports, whereas tunnels with portals below ground level are typical for sub-aqueous tunnels. Therefore, the additional dam above the tunnel portal was given the cross-section of a dike (Fig. 2).

The net wind pressure differences at the tunnel portals relative to the static pressure of the undisturbed surrounding airflow were measured in both tubes (corresponding to tunnel exit and - entrance). In these tests no additional mean longitudinal airflow in the tunnel tubes was reproduced, though, as is well known, flow out of or into a tunnel modifies the wind pressure distribution. So, strictly speaking, the experimental data apply to stagnating tunnel air, but it is felt that for statistical predictions they can serve as a reasonable approach, even if an airflow exists in the tunnel tube.

Another simplification concerns the wind velocity gradient. No attempt was made to reproduce it, the flow over the model therefore being uniform, except for the thin boundary layer close to the model plate. Hence the measured wind pressure data need only be related to the stagnation pressure $\frac{\rho}{2} v^2$ of the undisturbed incident flow to arrive at non-dimensional coefficients. Some difficulties can arise in applying them to full-scale in defining the relevant stagnation pressure (in the aerodynamics of buildings one resorts to appropriately forming a mean stagnation pressure over a certain height of the boundary layer).

The tests were performed at a wind tunnel speed of 30.3 m/s which corresponded to a Reynolds number, with the tunnel height taken as the characteristic length, $Re = v\,h/\nu = 9.5 \cdot 10^6$ (ν = kinematic viscosity). At this speed no dependence of the wind pressure coefficients on Reynolds number was observed. Because of the prevailing sharp edges of the model and prototype, the model flow is similar to full-scale flow. Hence the experimental data could be converted to full-scale conditions, though the smooth and open ground area in front of the model tunnel portal and the existing uniform airflow clearly limit their applicability

From the extensive experimental data only two sets of wind pressure curves are presented for a tunnel portal above and below ground level respectively*. Figure 3 shows the experimental wind pressure coefficient

$$c_{exp} = \Delta p_{exp} / \frac{\rho}{2} v^2 \qquad (1)$$

versus angle of wind incidence with respect to the tunnel axis. This is taken positive clockwise and counter-clockwise for right-hand and left-hand traffic respectively.

These diagrams illustrate two features. Firstly, the wind pressure curves for portals below ground level are rather similar to each other whether or not additional devices are present. Even the variation of th wind pressure coefficients with the portal shape is small if the portal with a light adaptation section is excluded. This is shown in Fig. 4 wher the maximum and minimum wind pressure coefficients are plotted. No such behaviour is found at portals above ground level, but this can be explained easily by their exposure to the wind. Secondly, a light adaptation section reduces the wind pressure coefficient to half or less compared to a portal without such a device.

---

* For the total set of the experimental data see appendix.

The total wind pressure difference at a tunnel tube results from adding the corresponding values at the tunnel ends. If the tunnel is straight and has the same portals and a similar surrounding area, curves such as shown in Fig. 5 are obtained with portals above and below ground level respectively (from Fig. 3).

3. LEAST-SQUARES APPROXIMATION

The similar and relatively smooth curves for the total wind pressure differences at tunnels with portals below ground level inspired us to approximate them by a simple function. It appeared that

$$c = \bar{c} \cos^2 \varphi \qquad (2)$$

resulted in the least mean square deviations. Here $\bar{c}$ is the mean wind pressure coefficient, and φ the angle of wind incidence with respect to the tunnel axis. $\bar{c}$, so to speak, comprises in bulk the aerodynamic effects of the tunnel geometry and surroundings. It is presented in Fig. 6.

Equation 2 expresses that the wind pressure differences are substantially due to the wind component in the tunnel direction. Similarly, the resistance of an extended ground roughness, e.g. of a fillet or overlapping plates, depends on the vertical component of the oncoming stream. For that very reason the wind pressure differences at a tunnel with portals at ground level, but without any additional devices, can be very well approximated by the function $\cos^2$ (Fig. 5a, full line; the asymmetry is caused by the existence of two tubes). But, as soon as additional devices, such as a dividing wall or a light adaptation section are added, these do govern the wind pressure dependence on wind incidence, resulting in larger deviations.

To make the deviations visible Fig. 7 was prepared. It shows the experimental data related to the appropriate mean wind pressure coefficient $\bar{c}$ for all models tested, and the approximating function $\cos^2 \varphi$.

For a probabilistic approach to wind action on tunnel ventilation, finer details of the wind pressure curves are certainly less important. Experience shows that the statistical aspects of a random quantity can be sufficiently treated by suitably representing the basic experimental data by simple analytical functions. Of course, the question arises whether Eq. 2, which is apparently suited for tunnels in a relatively open area, can be applied to portals with surrounding buildings also.

As regards this, experimental data of earlier wind tunnel tests on a projected special road tunnel were available. This two-bore tunnel is formed by superstructing a highway with habitations on a length of about 500 m (Fig. 8). In these tests the whole volume of existing and planned buildings was modelled in a zone of 500 m radius around the centre of the tunnel.

The experimental wind pressure differences at both tunnel tubes, related to the stagnation pressure of the wind, are shown in Fig. 9. Obviously, a $\cos^2$ approximation is suitable. The mean wind pressure coefficient amounts to $\bar{c} = 0.41$. In this diagram the wind pressure coefficients for a tunnel with portals below ground level were added for comparison.

Considering these experimental results it is felt that Eq. 2 can be applied to straight or moderately curved tunnels, if the tunnel portals do not lie in the wakefield of tall single buildings. In other words, for the present purpose a $\cos^2$ approximation of the dependence of the total wind pressure differences at a tunnel on the angle of wind incidence seems to be suitable, if the surrounding area is open, which as a rule is formed partly by the roadways, and/or has a varying topography.

If no experimental data are available, the mean wind pressure coefficient $\bar{c}$ can be estimated as follows: estimate the wind pressure difference at the tunnel for wind in the tunnel direction and relate it to the stagnation pressure of the causal wind velocity.

4. DISTRIBUTION OF WIND PRESSURE DIFFERENCES

We shall now combine the wind pressure differences at a tunnel with wind statistics. These are available practically for all places.

The density function of the wind velocity v is generally present as a step function of the wind strength in Bft. From experience it can be approximated by Rayleigh's density function

$$f_v(v)^* = \frac{\pi}{2} \frac{v}{\bar{v}^2} \exp\left[-\frac{\pi}{4}\left(\frac{v}{\bar{v}}\right)^2\right] , \qquad (3)$$

where $\bar{v}$ is the mean wind velocity.

Since the wind pressure varies with the square of the wind veloci

* $f_v(v)$ reads 'density function of v as a function of v'.

$$\Delta p = c(\varphi)\,\frac{\rho}{2}\,v^2 \quad , \tag{4}$$

the density function of all positive or negative wind pressure differences at a tunnel (positive or negative in regard to the normal direction of traffic flow/ventilation) can be written in the following form

$$f_{\Delta p}(\Delta p) = \frac{1}{4}\int_{\varphi=-\frac{\pi}{2}}^{+\frac{\pi}{2}} \frac{f_\psi(\psi)}{c\,\frac{\rho}{2}\,\bar{v}^2}\,\exp\left[-\frac{\pi}{4}\,\frac{\Delta p}{c\,\frac{\rho}{2}\,\bar{v}^2}\right] d\varphi \quad . \tag{5}$$

Here the wind pressure coefficient c is given by Eq. 2. $f_\psi(\psi)$ is the density function of wind directions ψ. The mean wind velocity $\bar{v}$ varies with ψ and therefore depends on φ. Wind statistics present it as the mean over the sector $\Delta\psi$ (generally $\frac{\pi}{4}$) around ψ. As an example Figure 10 shows the wind conditions (diurnal mean over a year) for a large German town.

The integration of Eq. 5 is carried out for $\Delta\psi$ with equally distributed $\bar{v}$ and for the frequency of occurrence of wind directions. Subsequent summation for all sectors $\Delta\psi$ with wind frequency P_ψ over the half-circle, the sector of positive or negative wind influence, yields

$$f_{\Delta p}(\Delta p) = \frac{1}{4}\sum_{\pi}\left(\frac{P_\psi}{\bar{c}\,\frac{\rho}{2}\,\bar{v}^2}\int_{\varphi_1}^{\varphi_1+\Delta\psi} \frac{\exp\left[-\frac{\pi}{4}\,\frac{\Delta p}{\bar{c}\,\frac{\rho}{2}\,\bar{v}^2}\,\frac{1}{\cos^2\varphi}\right]}{\cos^2\varphi}\,d\varphi\right) \quad . \tag{6}$$

The integration can easily be performed

$$f_{\Delta p}(\Delta p) = \frac{1}{2}\sum_{\pi}\left(\frac{P_\psi}{\sqrt{\bar{c}\,\frac{\rho}{2}\,\bar{v}^2\Delta p}}\,\exp\left[-\frac{\pi}{4}\,\frac{\Delta p}{\bar{c}\,\frac{\rho}{2}\,\bar{v}^2}\right]\Phi\left(\sqrt{\frac{\pi}{2}\,\frac{\Delta p}{\bar{c}\,\frac{\rho}{2}\,\bar{v}^2}}\,\mathrm{tg}\,\varphi\right)\Bigg|_{\varphi_1}^{\varphi_1+\Delta\psi}\right) , \tag{7}$$

where

$$\Phi(z) = \frac{1}{\sqrt{2\pi}}\int_{z_1}^{z_2}\exp\left(-\frac{\zeta^2}{2}\right)d\zeta$$

is the standardized normal distribution function.

Expressing the wind pressure difference Δp by the wind component in tunnel direction v_p :

$$\Delta p = \bar{c}\,\frac{\rho}{2}\,v_p^2 \quad , \tag{9}$$

the density function Eq. 7 can be written in the following form

$$f_{\Delta p}(v_p) = \sum_{\pi}\left(\frac{p_\psi}{\bar{v}} \exp\left[-\frac{\pi}{4}\left(\frac{v_p}{\bar{v}}\right)^2 \right] \Phi\left(\sqrt{\frac{\pi}{2}}\,\frac{v_p}{\bar{v}}\,\mathrm{tg}\,\varphi \right) \Bigg|_{\varphi_1}^{\varphi_1+\Delta\psi} \right) . \tag{10}$$

Since in this equation the properties of the wind action at a special tunnel, expressed by $\bar{c}$, do no longer appear, Eq. 10 can be compared with Rayleigh's density function of the wind velocities (Eq. 3). This is done in Fig. 11 using a mean velocity $\bar{v} = 3.66\ \frac{m}{s}$ for SW-wind, according to Fig. 10. Figure 11 shows Rayleigh's density function and the pressure density curves for wind within $\frac{\pi}{4}$ at a tunnel with its axis directed SSE $\left(\frac{\pi}{4} \leq \varphi \leq \frac{\pi}{2} \right)$ and SW $\left(-\frac{\pi}{8} \leq \varphi \leq \frac{\pi}{8} \right)$ respectively. The latter practically coincides with Rayleigh's density function because of the initially small influence of wind incidence on wind pressure for winds in the tunnel direction. Figure 11 also presents the stepped density function of the original wind data.

Assuming the same mean wind velocity for all directions with favourable or unfavourable wind influence, and the wind frequencies of occurrence to be equally distributed over the rhumb-card, Eq. 10 gives

$$f_{\Delta p}(v_p) = \frac{1}{\bar{v}_p} \exp\left[-\frac{\pi}{4}\left(\frac{v_p}{\bar{v}_p}\right)^2 \right] . \tag{1}$$

This resembles the normal density function and motivated us try to constitute a mean wind influence velocity $\bar{v}_p$ even for given wind conditions such that this function could replace the rather unwieldy formula Eq. 10. Obviously, this can be done by weighting the mean wind velocities from wind statistics in the following way:

$$\bar{v}_p = \frac{\sum_{\pi}\left(p_\psi\, \bar{v} \cos\varphi_m \right)}{\sum_{\pi}\left(p_\psi \cos\varphi_m \right)} . \tag{}$$

Here φ_m is the angle between the tunnel axis and the middle of $\Delta\psi$ in question with $\bar{v}$ and the pertinent wind frequency of occurrence P_ψ.

In Fig. 12 a comparison is made of the density function, as calculated from Eq. 11, and the exact density function Eq. 10. It is exact in the sense that statistical data from Fig. 10 were applied. The tunnel direction was chosen NS because of the lowest mean velocity for southerly winds (2.86 $\frac{m}{s}$; max. for west wind, 3.85 $\frac{m}{s}$).

In Fig. 12 the integral of Eq. 10 and the distribution function resulting from Eq. 11

$$F_{\Delta p} = 2\Phi\left(\sqrt{\frac{\pi}{2}}\,\frac{v_p}{\bar{v}_p}\right) - 1 \qquad (13)$$

where *

$$\Phi(z) = \frac{1}{\sqrt{2\pi}} \int_{-\infty}^{z} \exp\left(-\frac{\zeta^2}{2}\right) d\zeta \quad . \qquad (14)$$

are presented on probability paper. From this it is seen that the exact wind pressure distribution curve follows rather closely the modified normal distribution function. The respective value of the mean wind influence velocity is (for $F_{\Delta p} \leq .95$) 3.11 $\frac{m}{s}$, whereas the weighted $\bar{v}_p$ amounts to 3.25 $\frac{m}{s}$, the deviation being only 4.5 %.

In conclusion we note that the density curve of wind pressure differences at a tunnel - as a function of the wind influence velocity v_p - can be approximated by a modified normal density function with different mean wind influence velocities $\bar{v}_{p+}$ and $\bar{v}_{p-}$ for favourable and unfavourable winds. Consequently, the distribution of all pressure differences caused by wind (including calms) is given by

$$F_{\Delta p,\,total} = P_{\psi+}\left[2\Phi\left(\sqrt{\frac{\pi}{2}}\,\frac{v_p}{\bar{v}_{p+}}\right) - 1\right] + P_{\psi-}\left[2\Phi\left(\sqrt{\frac{\pi}{2}}\,\frac{v_p}{\bar{v}_{p-}}\right) - 1\right] + P_{calms} \quad , \qquad (1$$

where $P_{\psi+}$, $P_{\psi-}$, P_{calms} is the probability of occurrence of favourable and unfavourable winds, and calms respectively.

5. APPLICATION TO LONGITUDINAL VENTILATION

The interrelationship between tunnel ventilation, influence of

* From now on the common formula for the normal distribution function is chosen.

traffic flow , and wind pressure differences is expressed by the equation of momentum. For a tunnel with one-way traffic having a constant cross-section and being ventilated by axial fans, it is written as

$$n_j \rho Q_j (v_j - v_t) + \text{sign}(v_c - v_t)\, n_c \overline{c_c A_c}\, \frac{\rho}{2} (v_c - v_t)^2 - \\ - \zeta_t \frac{\rho}{2} v_t^2 A_t + \text{sign}\left(\begin{smallmatrix}\text{wind}\\ \text{influence}\end{smallmatrix}\right) c \frac{\rho}{2} v^2 A_t = 0 \qquad (16)$$

where sign (wind influence) = -1 for retarding wind pressure. From Eq.16 it is seen that

$$\Delta n_j = \frac{c \frac{\rho}{2} v^2 A_t}{\rho Q_j (v_j - v_t)} \qquad (17)$$

additional fans are necessary to maintain certain air conditions, if the traffic situation is regarded as being unchanged.

With Eq. 9 we get

$$\Delta n_j = \frac{1}{C} \left(\frac{v_p}{\bar{v}_p} \right)^2 , \qquad (18)$$

where

$$C = \frac{\rho Q_j (v_j - v_t)}{\bar{c} \frac{\rho}{2} \bar{v}_p^2 A_t} \qquad (19)$$

is a non-dimensional quantity for the sake of abbreviation.

Considering the same traffic situation over a sufficiently long period, it follows from Eqs. 11 and 18 that the density function of additional fans to cope with the wind action is given by

$$f_{\Delta n_j}(\Delta n_j) = \frac{1}{2} \sqrt{\frac{C}{\Delta n_j}} \exp\left[-\frac{\pi}{4} C \Delta n_j \right] . \qquad (20$$

The corresponding distribution function takes the form

$$F_{\Delta n_j} = 2\Phi\left(\sqrt{\frac{\pi}{2} C \Delta n_j} \right) - 1 . \qquad (2$$

Hence, the probability that a desired air quality can be maintained with $\Delta N_j \leq \Delta n_j$ additional fans is:

$$P\left(\Delta N_j \leq \Delta n_j \,/\, \begin{smallmatrix}\text{retarding}\\ \text{wind pressure}\end{smallmatrix}\right) = 2\Phi\left(\sqrt{\frac{\pi}{2} C \Delta n_j} \right) - 1 , \qquad (2$$

The same relationship holds for light obscuration by Diesel smoke (or other criteria), if the Diesel exhaust is taken instead of carbon monoxide.

In the following the non-dimensional quantities

$$\zeta_c = \bar{\alpha}\, n_{c,max} \,, \qquad \zeta_p = \bar{c}\left(\frac{\bar{v}_p}{v_c}\right)^2 \tag{27}$$

have been introduced, where $n_{c,max}$ is the maximum number of vehicles in the tunnel (traffic peak). Moreover, the non-dimensional variables

$$\mu = v_p / \bar{v}_p \,, \qquad \nu = n_c / n_{c,max} \,, \qquad \sigma = co / co_i \tag{28}$$

are used. Here

$$co_i = \frac{\bar{Q}_{co}\, n_{c,max}}{A_t v_c} \tag{29}$$

is the CO-concentration at the tunnel exit, if the tunnel air would stream with the speed of traffic flow.

Hence, Eq. (26) reduces to the non-dimensional form

$$\sigma = \frac{\left(\frac{\zeta_t}{\zeta_c} - \nu\right)\nu}{\sqrt{\nu^2 - \left(\frac{\zeta_t}{\zeta_c} - \nu\right)\left(\frac{\zeta_p}{\zeta_c}\mu^2 - \nu\right)} - \nu} \,. \tag{30}$$

From this we get for $\mu = 0$ (no wind influence)

$$\sigma\,(\mu = 0) = \nu + \sqrt{\frac{\zeta_t}{\zeta_c}\,\nu} \,. \tag{31}$$

Resolving Eq. 30 for μ gives

$$\mu = \left[\left(\frac{\nu^2}{\sigma^2} - \frac{\nu}{\sigma}\left(2 + \frac{1}{\sigma}\frac{\zeta_t}{\zeta_c}\right) + 1\right)\nu\,\frac{\zeta_c}{\zeta_p}\right]^{\frac{1}{2}} \,. \tag{32}$$

Finally, the CO concentration arising at traffic peak ($\nu = 1$) without any wind influence ($\mu = 0$) is introduced:

or in terms of the complementary probability

$$P\left(\Delta N_j \geq \Delta n_j \,/^{\text{retarding}}_{\text{wind pressure}}\right) = 2\left(1 - \phi\left(\sqrt{\tfrac{\pi}{2} C \Delta n_j}\right)\right) . \qquad (23)$$

If instead the left-hand side of Eq. 23 is given, the additional ventilation boost needed is obtained immediately.

For longitudinally ventilated tunnels, depending on traffic conditions, there always exists a certain retarding wind pressure above which fewer fans are needed when the flow direction is changed. From Eq. 23 it can be decided easily whether interchangeable axial fans are of advantage.

In the case where there is no reserve margin in ventilation boost or if the ventilation plant fails, the question is how often and to what extent the concentration of carbon monoxide CO might exceed required limits. This can be answered readily by inserting

$$co = \frac{\bar{Q}_{CO}\, n_c}{v_t\, A_t} \qquad (24)$$

as a function of $v_p/\bar{v}_p$ with the help of the momentum equation (Eq. 16) into Eq. 13. Here $\bar{Q}_{CO}$ is the mean volume flow rate of carbon monoxide exhaust of a vehicle.

A more complex task is the evaluation of the air quality in the tunnel tube or at the tunnel ends, if in addition to the wind a variation of traffic density is allowed for, whereby the speed is assumed to be constant. This proves correct for normal traffic conditions. In addition, it is supposed that the tunnel is ventilated by the passing vehicles only.

From the momentum equation (Eq. 16) the mean velocity of airflow in the tunnel is given by

$$v_t = \frac{\sqrt{(n_c \bar{\alpha} v_c)^2 - (\zeta_t - n_c \bar{\alpha})(\bar{c} v_p^2 - n_c \bar{\alpha} v_c^2)} - n_c \bar{\alpha} v_c}{\zeta_t - n_c \bar{\alpha}} , \qquad (2$$

where $\bar{\alpha} = \overline{c_c A_c}/A_t$ is the mean drag area of a vehicle inside the tunr related to the tunnel cross-sectional area. Inserting this in Eq. 24 we obtain

$$co = \frac{\bar{Q}_{CO}}{A_t} \frac{(\zeta_t - n_c \bar{\alpha})\, n_c}{\sqrt{(n_c \bar{\alpha} v_c)^2 - (\zeta_t - n_c \bar{\alpha})(\bar{c} v_p^2 - n_c \bar{\alpha} v_c^2)} - n_c \bar{\alpha} v_c} . \qquad (2$$

$$co_d = \frac{\bar{Q}_{CO}\, n_{c,max}}{A_t\, v_{t,max}} \tag{33}$$

or as a non-dimensional quantity

$$\sigma_d = \frac{co_d}{co_i} = \sigma\,(\nu = 1,\ \mu = 0) = \frac{v_c}{v_{t,max}} \quad . \tag{34}$$

Here

$$\frac{v_{t,max}}{v_c} = 1\Big/\left(1 + \sqrt{\frac{\zeta_1}{\zeta_c}}\right) \tag{35}$$

is the maximum air stream velocity in the tunnel related to the traffic speed.

If wind and traffic are mutually exclusive, the distribution function of the CO concentration at the tunnel exit is given by

$$F_{CO} = \int_{n_c}\int_{v_p} f_{n_c}(n_c)\, f_{\Delta p}(v_p)\, dn_c\, dv_p \quad , \tag{36}$$

where $f_{\Delta p}$ is the readily known wind pressure density function and f_{n_c} the traffic density function. (Actually traffic density and wind conditions are not fully mutually exclusive. So the morning traffic peak coincides with periods of weak winds; but this can be neglected here.)

Experience shows that uninterrupted normal traffic flow is as a rule equally distributed, if it is arranged as a function of traffic flow. Hence constant density for the number of vehicles in the tunnel is assumed in the present example:

$$f_{n_c}(n_c) = \frac{1}{n_{c,max}} \quad , \tag{37}$$

or in non-dimensional form

$$f_{n_c}(\nu) = 1 \quad . \tag{38}$$

Inserting this, and the non-dimensional wind pressure density function (from Eq. 11)

$$f_{\Delta p}(\mu) = \exp\left(-\frac{\pi}{4}\mu^2\right) \tag{39}$$

into Eq. 36 we have

$$F_{CO} = \int_{\nu} \int_{\mu} \exp\left(-\frac{\pi}{4}\mu^2\right) d\nu \, d\mu \quad . \tag{40}$$

Finally, substitution of μ by σ from Eq. 32 and subsequent differentiation with respect to σ yields the density function of the CO concentration at the tunnel exit

$$f_{CO}(co) = \frac{A_t v_c}{\bar{Q}_{CO} n_{c,max}} \sqrt{\frac{\zeta_c}{\zeta_p}} \int_{\nu=0}^{\substack{1 \text{ for } co/co_d \geq 1 \\ \nu(\sigma) \text{ for } co/co_d < 1}} \exp\left[-\frac{\pi}{4}\frac{\zeta_c}{\zeta_p}\nu\left(\frac{\nu^2}{\sigma^2} - \frac{\nu}{\sigma}\left(2+\frac{1}{\sigma}\frac{\zeta_t}{\zeta_c}\right)+1\right)\right] \frac{\sqrt{\nu}}{\sigma} \frac{\frac{\nu^2}{\sigma^2} - \frac{\nu}{\sigma}\left(1+\frac{1}{\sigma}\frac{\zeta_t}{\zeta_c}\right)}{\left[\frac{\nu^2}{\sigma^2} - \frac{\nu}{\sigma}\left(2+\frac{1}{\sigma}\frac{\zeta_t}{\zeta_c}\right)+1\right]^{\frac{1}{2}}} d\nu \tag{41}$$

The integration area is shown in Fig. 13. The upper limit of integration is:

$$co \geq co_d : \quad \nu = 1 \, ,$$

$$co < co_d : \quad \nu = \nu(\mu=0) = \sigma + \frac{1}{2}\frac{\zeta_t}{\zeta_c} - \sqrt{\left(\sigma+\frac{1}{2}\frac{\zeta_t}{\zeta_c}\right)^2 - \sigma^2} \, . \tag{42}$$

Equation 41 must be solved numerically. Instead, the distribution function

$$F_{CO} = \int_{\nu=0}^{\substack{1 \text{ for } co/co_d \geq 1 \\ \nu(\sigma) \text{ for } co/co_d < 1}} \left[2\Phi\left(\sqrt{\frac{\pi}{2}\frac{\zeta_c}{\zeta_p}\nu\left(\frac{\nu^2}{\sigma^2} - \frac{\nu}{\sigma}\left(2+\frac{1}{\sigma}\frac{\zeta_t}{\zeta_c}\right)+1\right)}\right) - 1\right] d\nu \tag{43}$$

can be computed with less effort, the density function being found by differentiation. Here Φ from Eq. 14 is the normal distribution function. Besides, a quick survey of the distribution of the CO concentration can be obtained by counting out the density volume under curves co = const in Fig. 13.

We applied the density function of CO concentrations to the earlier tunnel with the highway superstructure, assuming normal traffic and ventilation by piston effect of the vehicles. Here the CO level at the flats of residents close to the tunnel ends is of primary interest.

The tunnel data are found in Fig. 13.

Two cases were computed: Mixed traffic with 15 % trucks and buses - these are assumed to be driven by Diesel engines - as common on week-days, and Sunday traffic with a negligible fraction of vehicles with Diesel engines. Results are shown in Fig. 14.

Finally, it should be pointed out that the statistical wind data employed must be carefully related to the actual problem to make reasonable predictions. The preceding example was based on long-term diurnal mean wind conditions. Hence Fig. 14 expresses the CO level over years. From this it could be judged immediately how long the tunnel in question must be ventilated mechanically under normal traffic conditions to observe a certain CO concentration limit. However, from this figure it cannot be estimated whether or not the respective CO concentrations would be admissible in the flats of residents living close to the tunnel exit, because no information is given on their duration. This could be done readily, if statistical data of wind duration were available. Besides, special problems can arise which demand the distribution of extremes in regard to wind conditions. But, if the actual wind data follow Rayleigh's density function, this probabilistic approach to the influence of wind on tunnel ventilation can be applied.

6. CONCLUSIONS

It has been shown that the density curve of the wind pressure differences at road tunnels, expressed by the wind component in tunnel direction, follow closely a modified normal density function under certain topographical conditions. This result is based on wind tunnel tests on some generic shapes of road tunnel portals. It appeared that the wind pressure differences along a tunnel can be approximated sufficiently by the $\cos^2$ of the angle of wind incidence with respect to the tunnel axis. The geometry of the tunnel ends and the topography of the surrounding area are accounted for by a mean wind pressure coefficient. For lack of experimental data, the wind pressure coefficient for wind in the tunnel direction can be taken as an approach. The experimental data in this paper can also serve as a guideline.

Two examples of application are provided. Predictions are made of the additional fan boost needed when critical traffic situations coincide with unfavourable winds, and the statistical behaviour of the CO level at the exit of a tunnel under normal traffic conditions is calculated.

The adequacy of the theoretical predictions of wind influence on tunnel ventilation provided by this paper will depend to a large extent on the selection of the correct statistical wind and traffic data. The topographical conditions at the tunnel portals should also be carefully accounted for. If this is considered, the analysis presented gains practical value in the tunnel ventilation system design process.

For several years I have repeatedly been engaged in the ventilation of vehicle tunnels. More than once the question arose to what extent the influence of wind on road tunnel ventilation should be considered in the tunnel ventilation system design. Wind is a statistical quantity, and therefore it was quite normal to treat tunnel ventilation under wind influence with statistical means.

To my knowledge this is the first attempt to cope with the problem. Therefore I regret I cannot refer to related work. The statistical relationships used in this paper can be looked up in any textbook on statistics; tables of the normal distribution function (Eq. 14) should be available there.

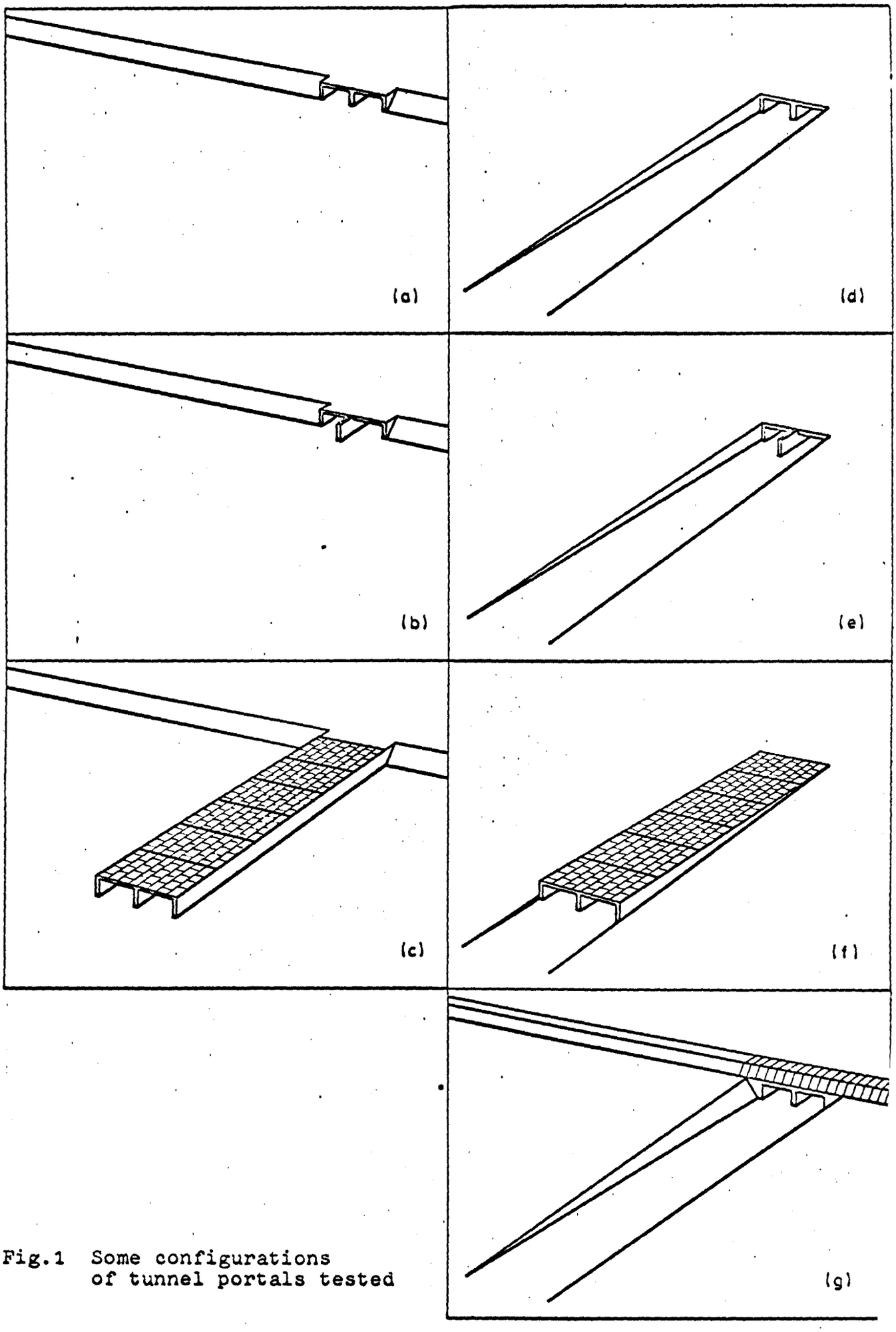

Fig.1 Some configurations of tunnel portals tested

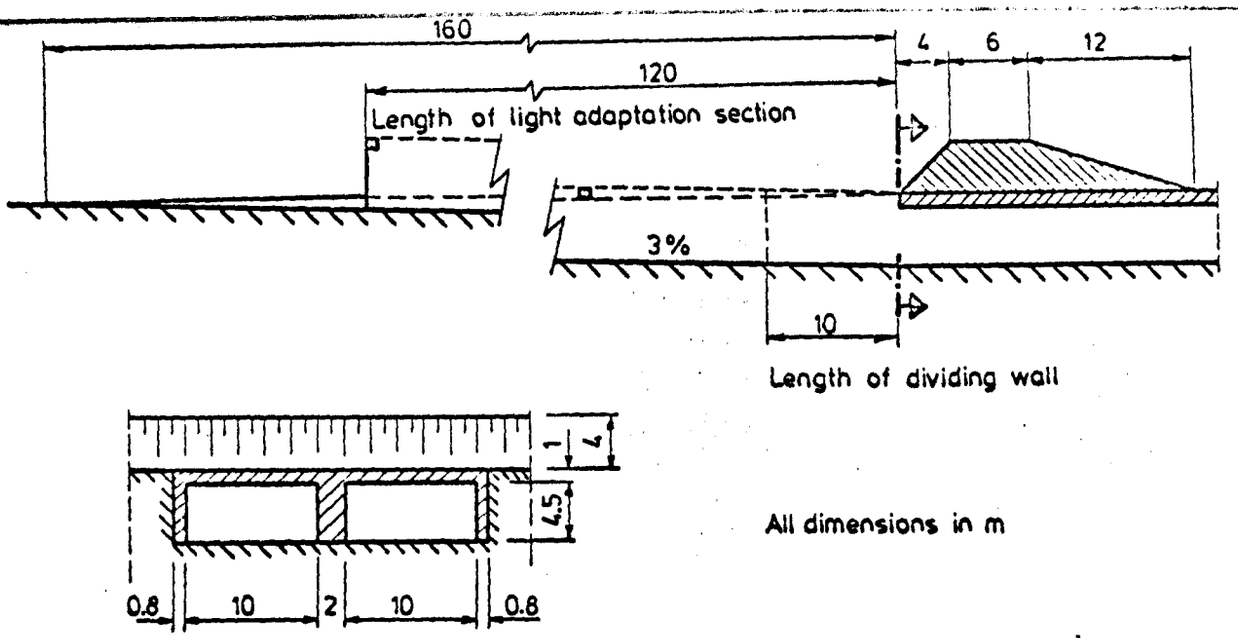

Fig.2 Plan of tunnel portal tested

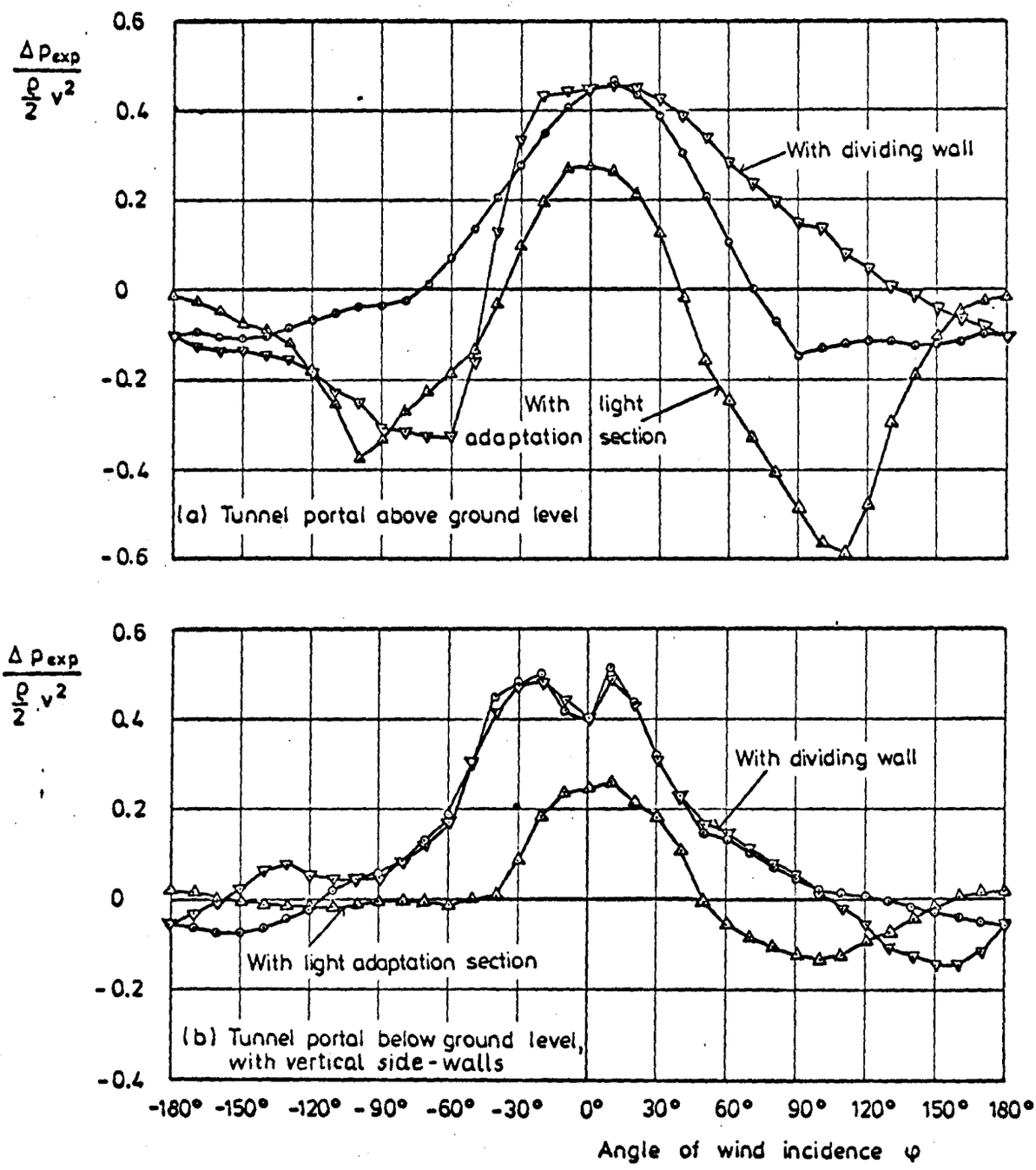

Fig.3 Wind pressure differences at a tunnel portal

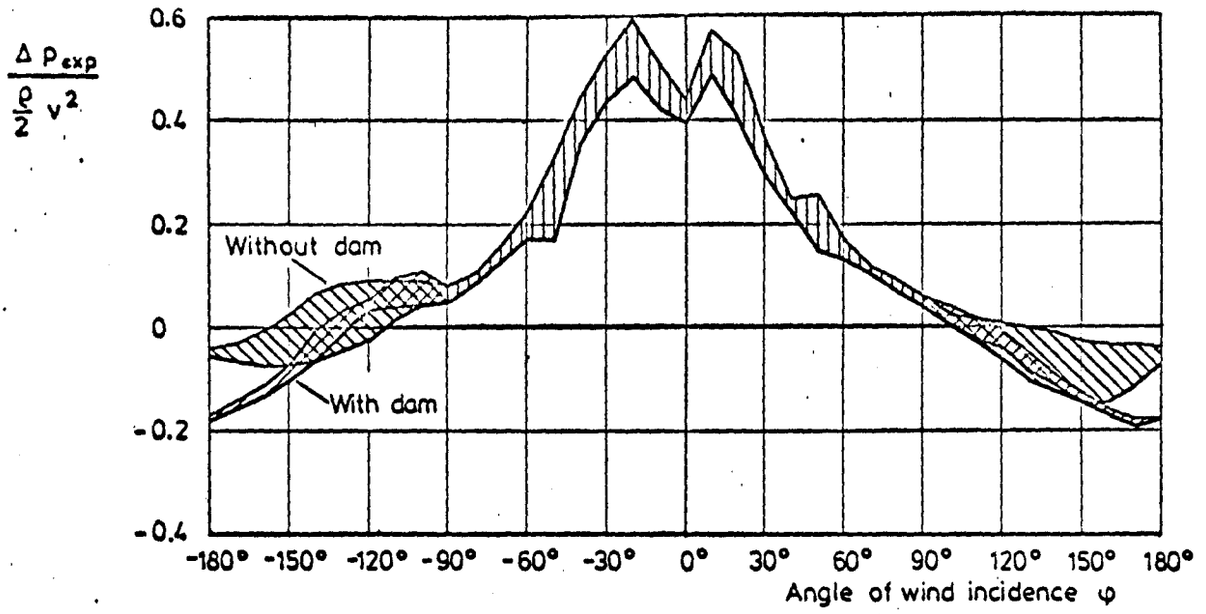

Fig.4 Maximum and minimum wind pressure differences at the tested tunnel portals below ground level, excepting portal with light adaptation section

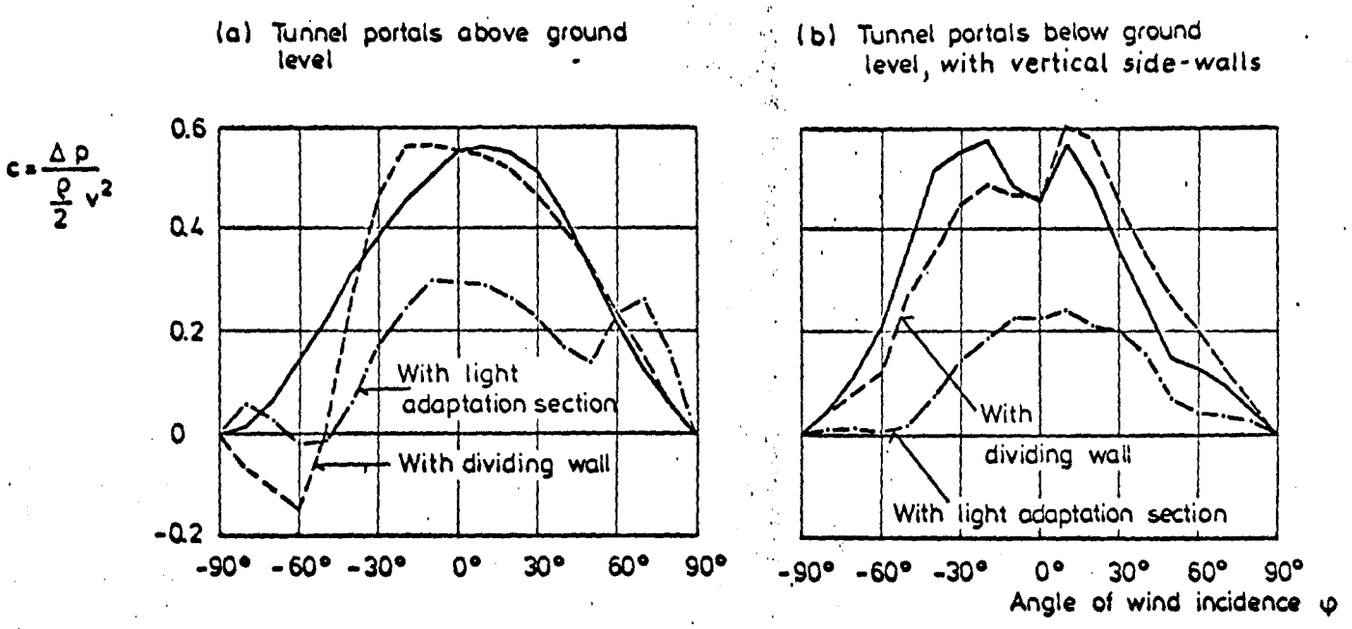

Fig.5 Coefficient of wind pressure difference along a tunnel

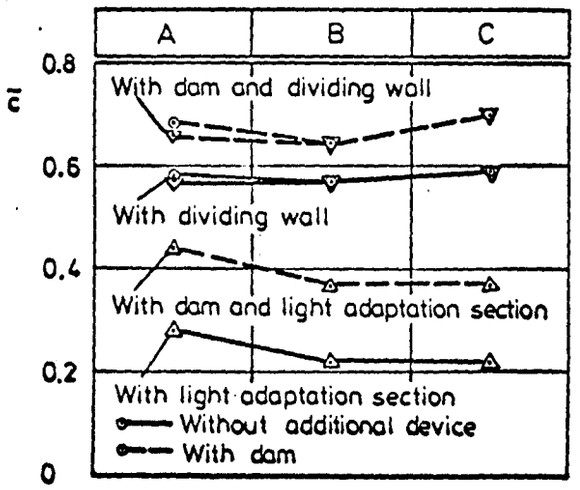

- A Portals above ground level
- B Portals below ground level, with vertical side-walls
- C Portals below ground level, with sloping bounds

Fig.6 Mean wind pressure coefficien for tunnels with portals tested

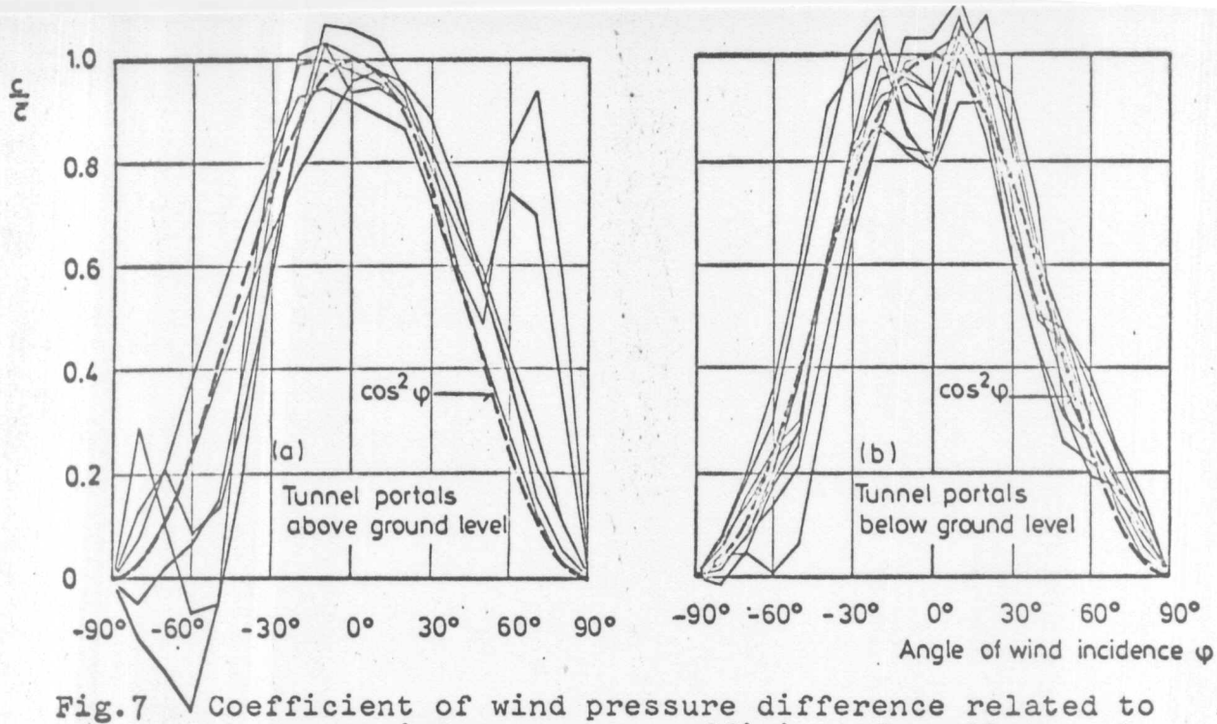

Fig.7 Coefficient of wind pressure difference related to the mean wind pressure coefficient for all tunnels tested, and the approximating function $\cos^2\varphi$

Fig.8 Wind tunnel model of a highway superstructure and the surrounding area

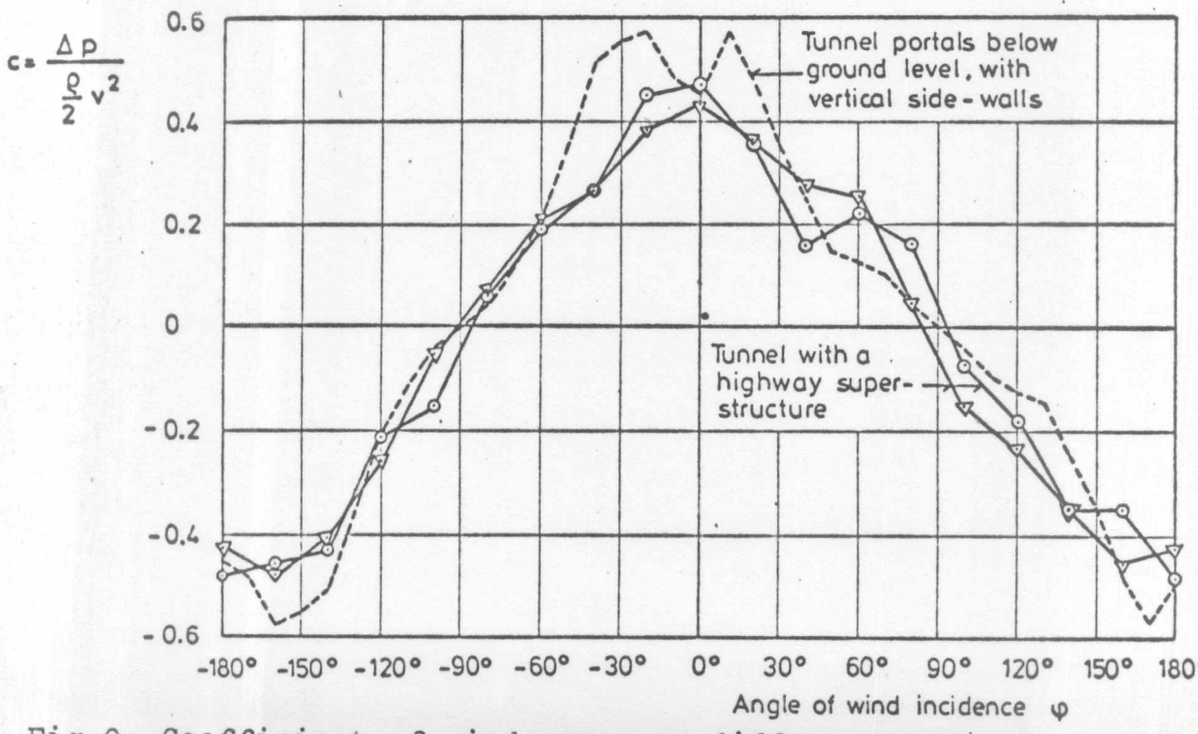

Fig.9 Coefficient of wind pressure differences at the tunnel with the highway superstructure and, for comparison, at a tunnel below ground level, with vertical side-walls

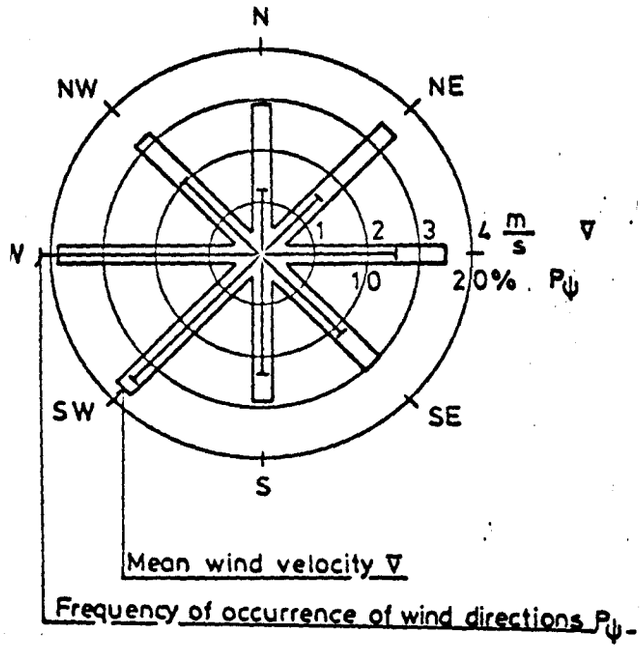

Fig.10 Example of long period diurnal mean wind statistics

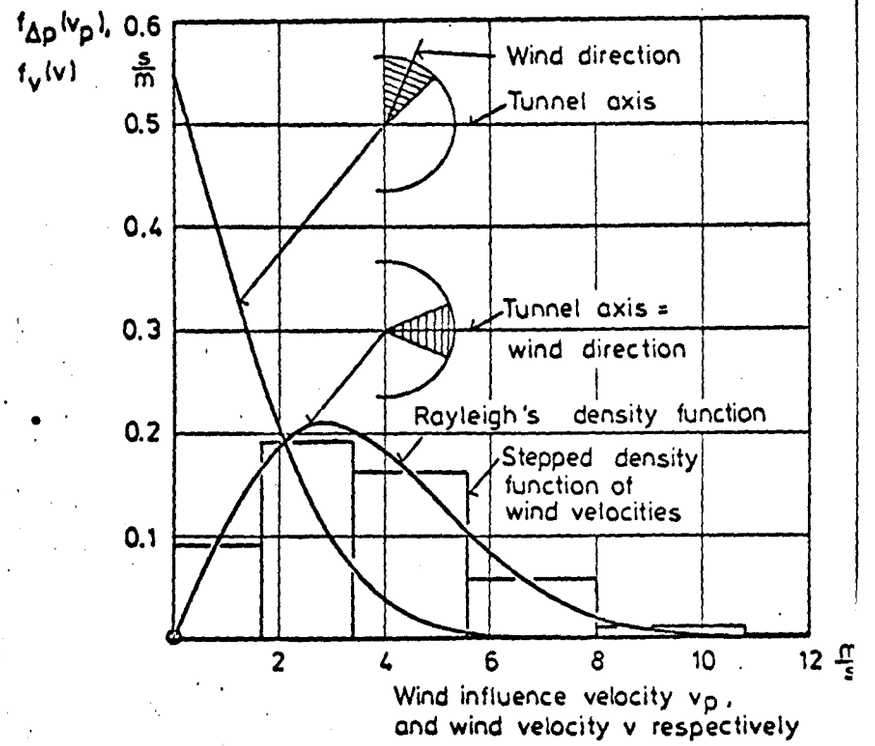

Fig.11 Comparison of wind pressure density curves for two different influence sectors of $\frac{\pi}{4}$ with Rayleigh's density function of wind velocities

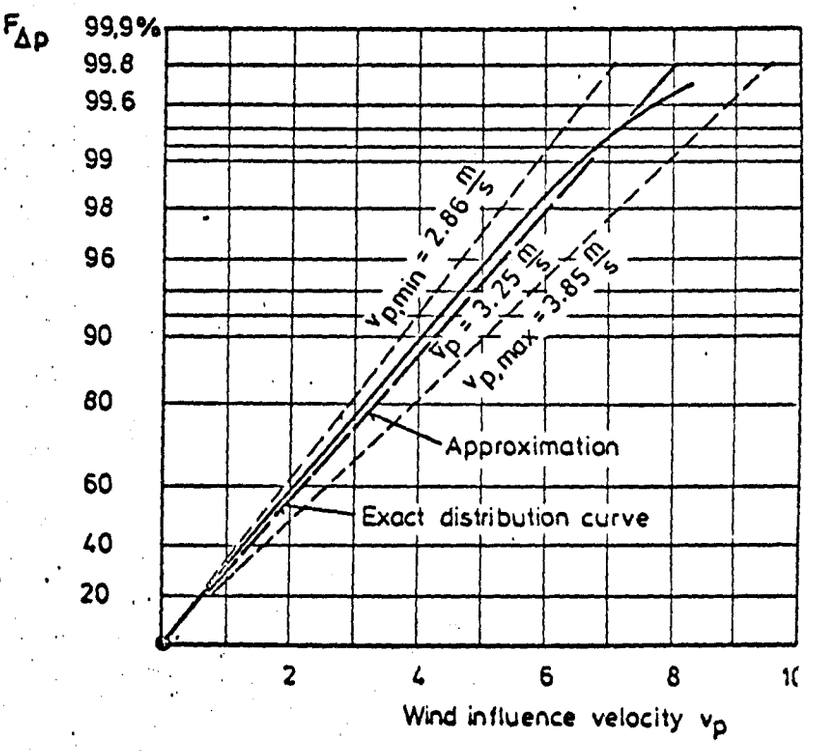

Fig.12 Comparison of wind pressure distribution curve with the modified normal distribution function

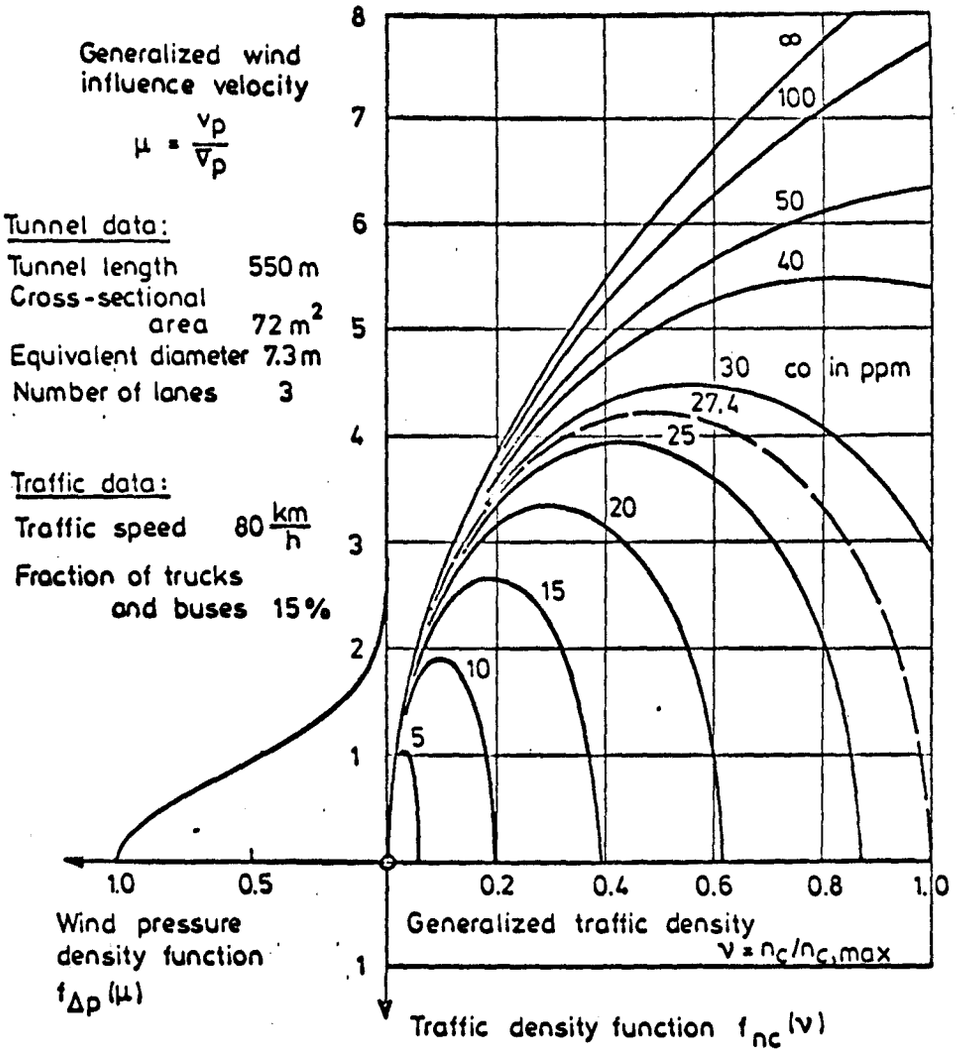

Fig.13 Example of the interrelationship between CO-concentration at tunnel exit, wind pressure, and traffic density for normal traffic conditions

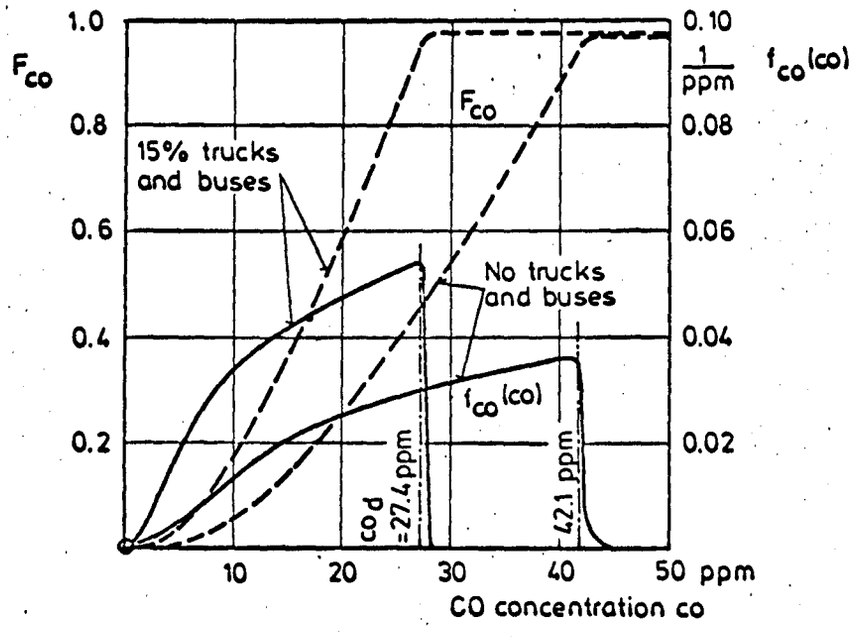

Fig.14 Density curve and distribution curve of CO-concentrations at the exit of the tunnel with the highway superstructure, under normal traffic conditions

7. APPENDIX

Wind pressure differences at the tunnel portals tested, related to the stagnation pressure of the undisturbed incident flow, $\Delta p_{exp}/\frac{\rho}{2} v^2$, versus angle of wind incidence with respect to the tunnel axis.

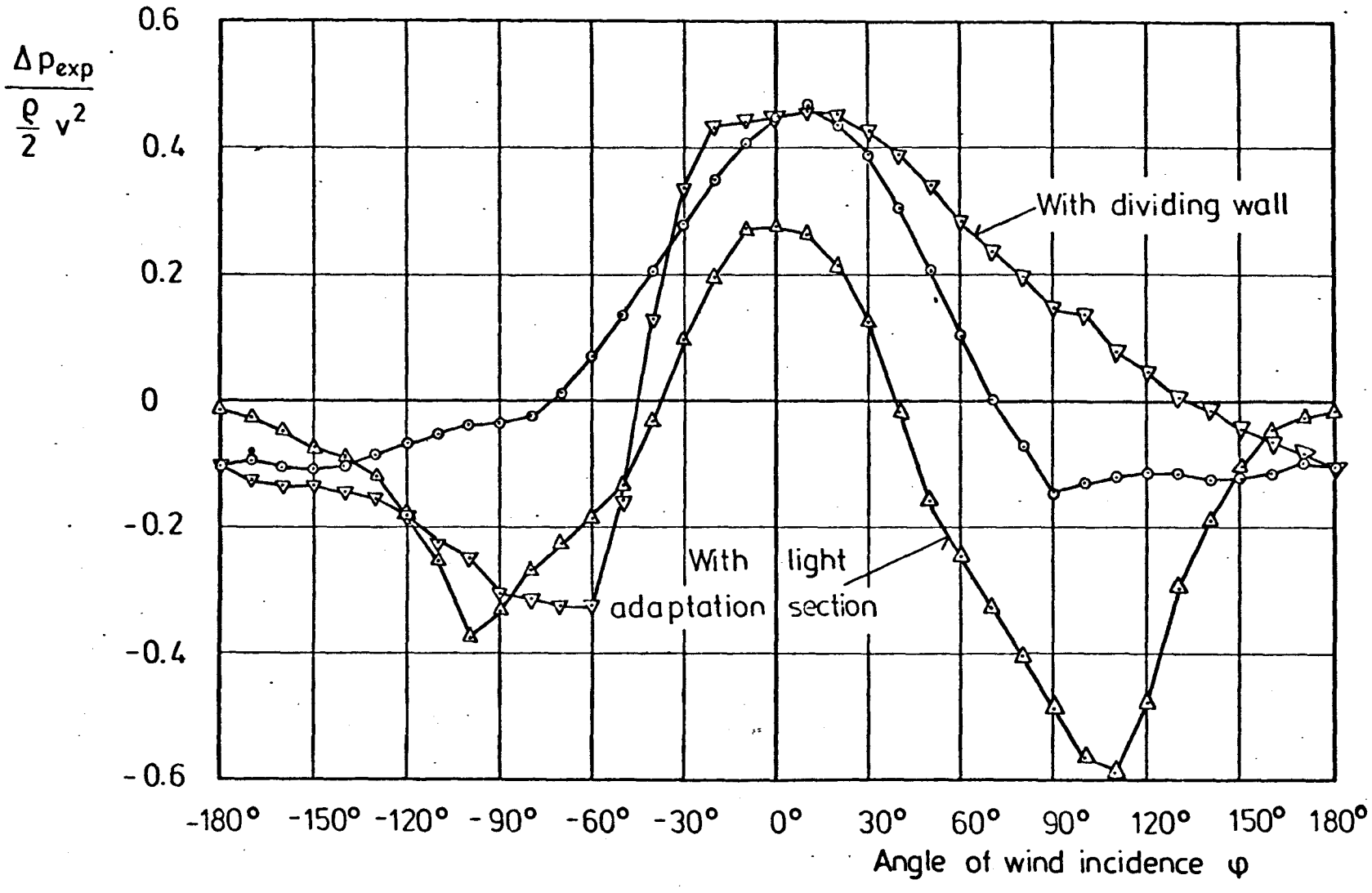

Fig. A1 Tunnel portal above ground level

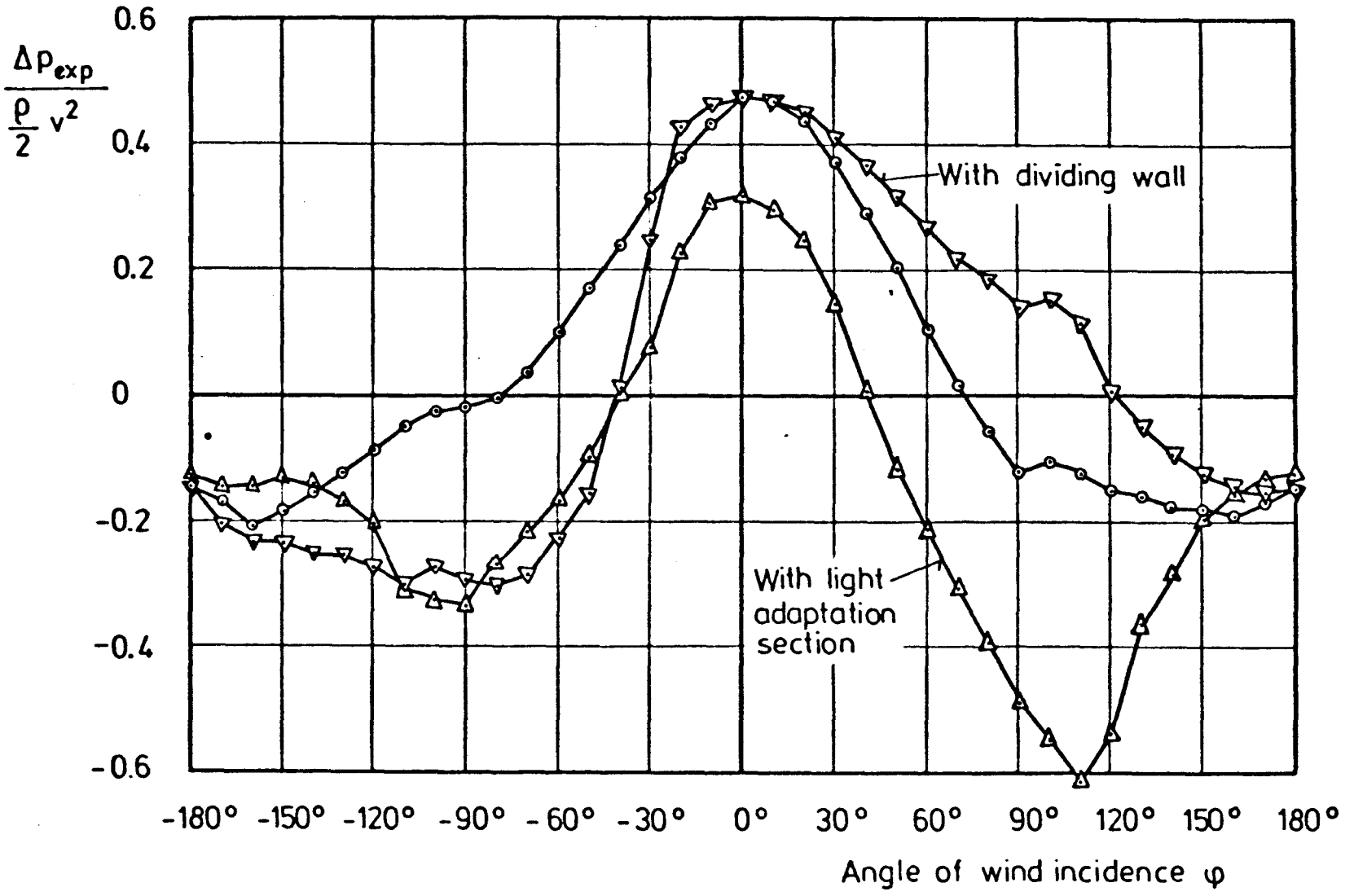

Fig. A2 Tunnel portal above ground level, with transverse dam above the tunnel end

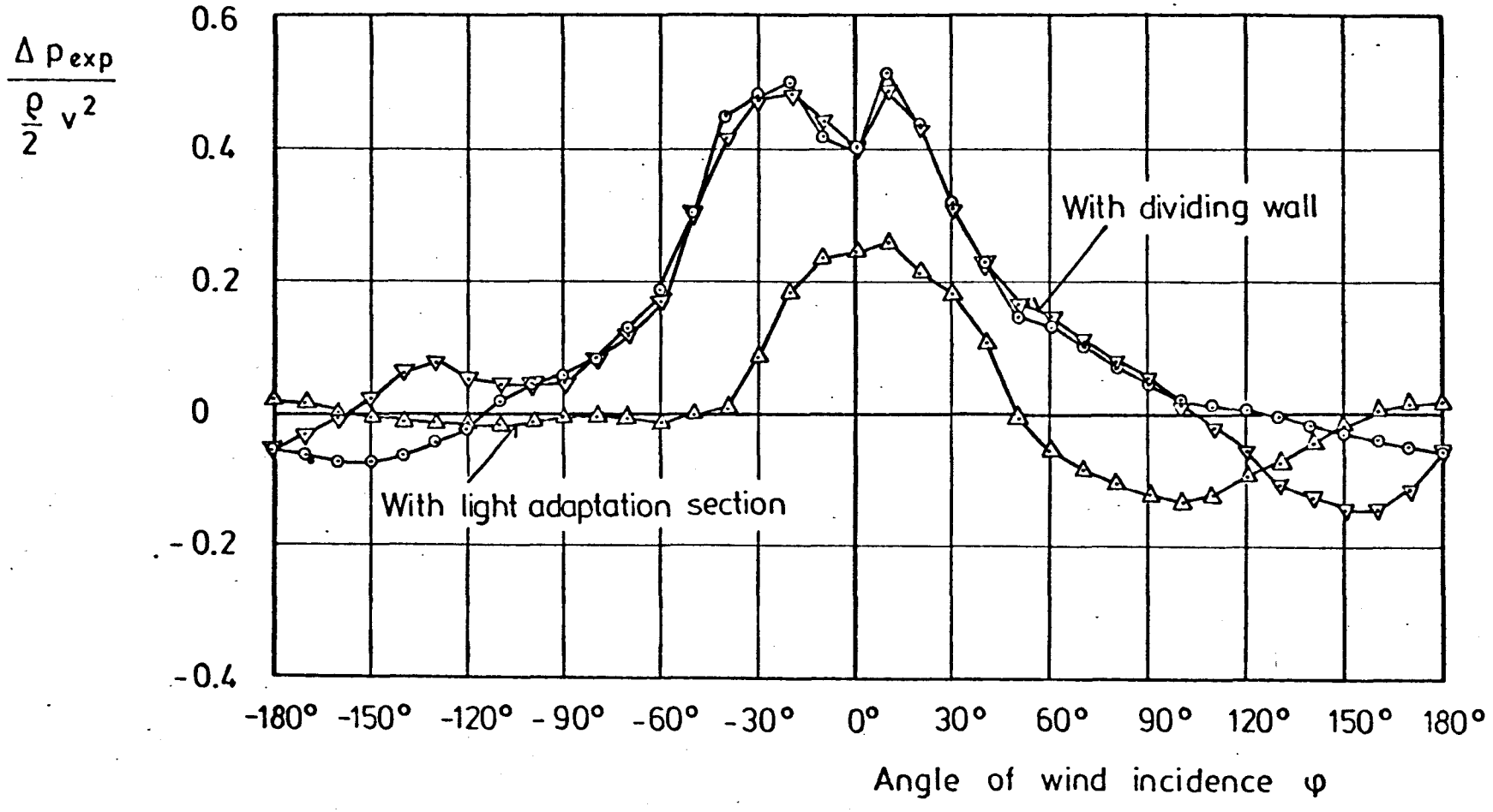

Fig. A3 Tunnel portal below ground level, with vertical side-walls

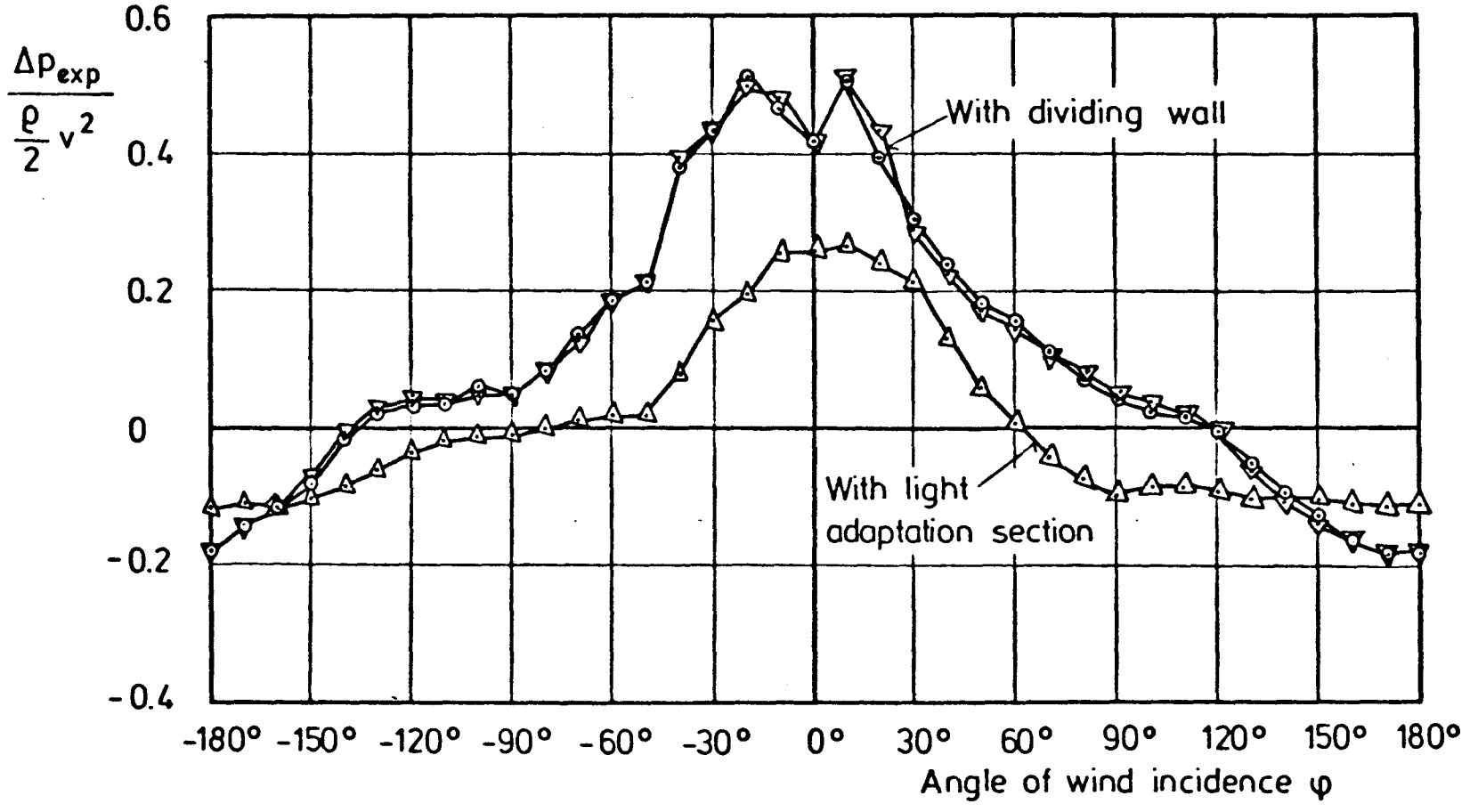

Fig. A4 Tunnel portal below ground level, with vertical side-walls, transverse dam above the tunnel end

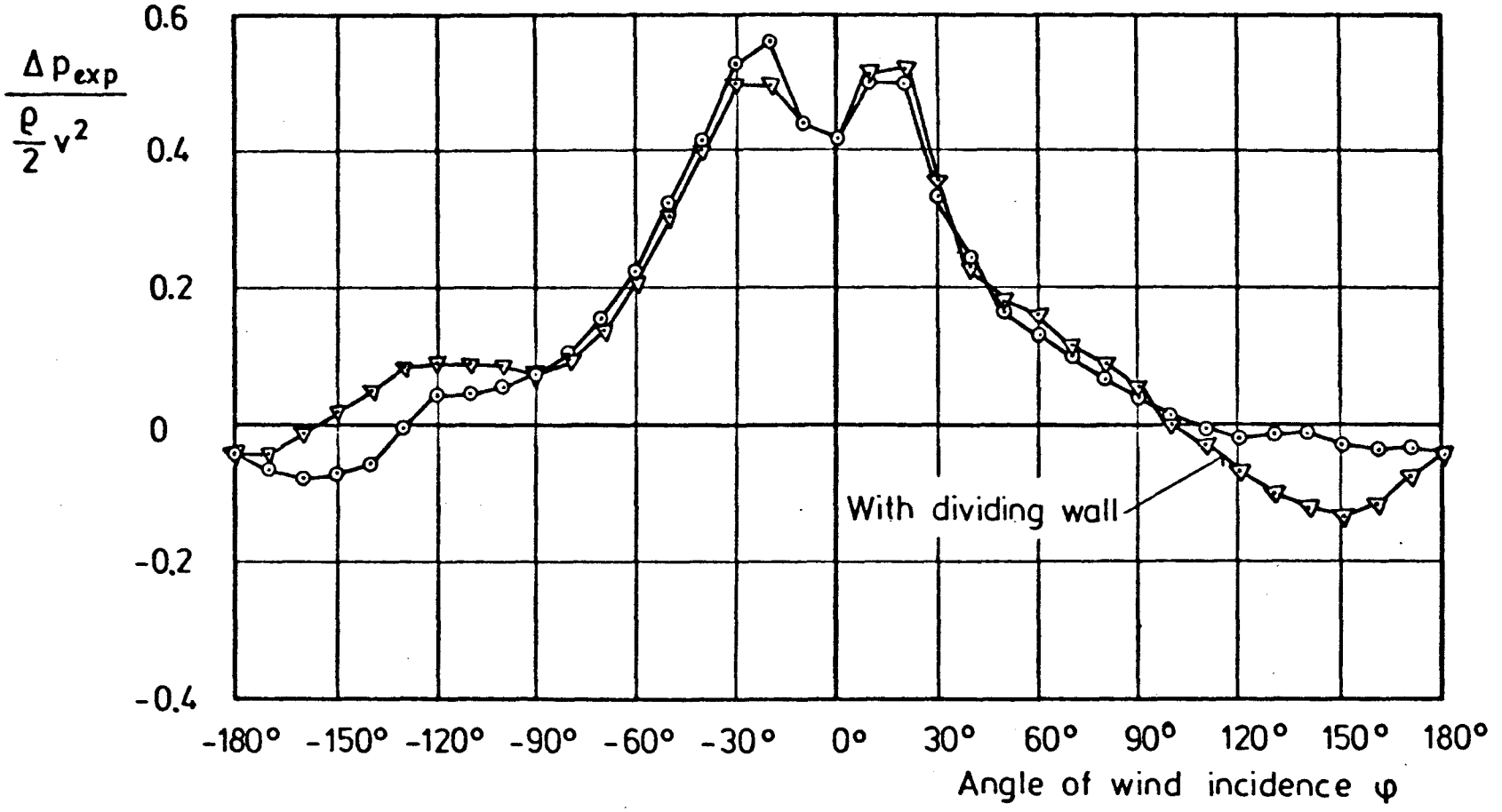

Fig. A5 Tunnel portal below ground level, with sloping bounds

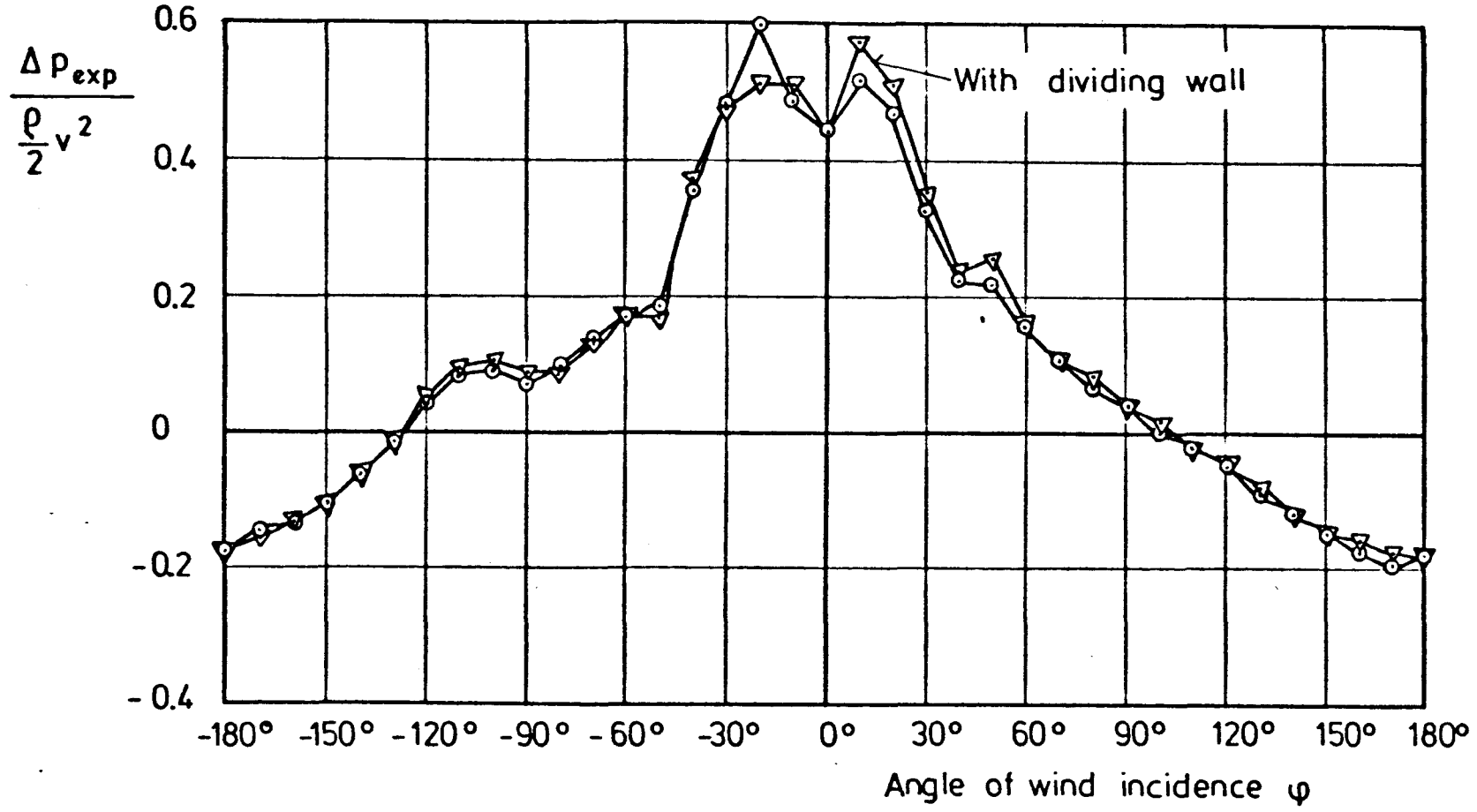

Fig. A6 Tunnel portal below ground level, with sloping bounds, transverse dam above the tunnel end